

1 **Transcriptomic responses of Antarctic clam *Laternula elliptica* to nanoparticles, at single and**
2 **combined exposures: revealing ecologically relevant biomarkers**

3

4 Rodolfo Rondon^{1*}, Catalina Valdés¹, Céline Cosseau², Elisa Bergami^{3,4}, César Antonio Cárdenas^{1,5},
5 Teresa Balbi⁶, Carolina Pérez-Toledo¹, Ignacio Garrido^{7,8}, Garance Perrois^{1,9}, Cristian Chaparro²,
6 Erwan Corre¹⁰, Ilaria Corsi³ and Marcelo González-Aravena¹

7

8 ¹ Departamento Científico, Instituto Antártico Chileno, Punta Arenas, Chile

9 ² Laboratoire des Interactions Hôtes-Pathogènes-Environnement, CNRS, IFREMER, Université de
10 Montpellier, Université de Perpignan « *Via Domitia* », Perpignan, France

11 ³ Department of Physical Science, Earth and Environment, Università di Siena, Siena, Italy

12 ⁴ Department of Life Sciences, University of Modena and Reggio Emilia, Via Giuseppe Campi 213/D,
13 Modena, Italy

14 ⁵ Millennium Institute Biodiversity of Antarctic and Subantarctic Ecosystems, Santiago, Chile

15 ⁶ Department of Earth Environment & Life Sciences, University of Genoa, Genoa, Italy

16 ⁷ Centro de Investigaciones Dinámica de Ecosistemas Marinos de Altas Latitudes, Valdivia, Chile

17 ⁸ Instituto de Ciencias Marinas y Limnológicas, Facultad de Ciencias, Universidad Austral de Chile,
18 Valdivia, Chile

19 ⁹ Tropical & Subtropical Research Center, Korea Institute of Ocean Science and Technology,
20 Busan, South Korea

21 ¹⁰ Faculté de Sciences, CNRS, FR 2424 CNRS, ABIMS, Station Biologique de Roscoff, Université
22 Sorbonne, Roscoff, France

23

24 * Corresponding author: Rodolfo Rondon; rrondon@inach.cl ; Plaza Muñoz Gamero 1055, Punta
25 Arenas 6200000, Chile.

26

27 **Highlights**

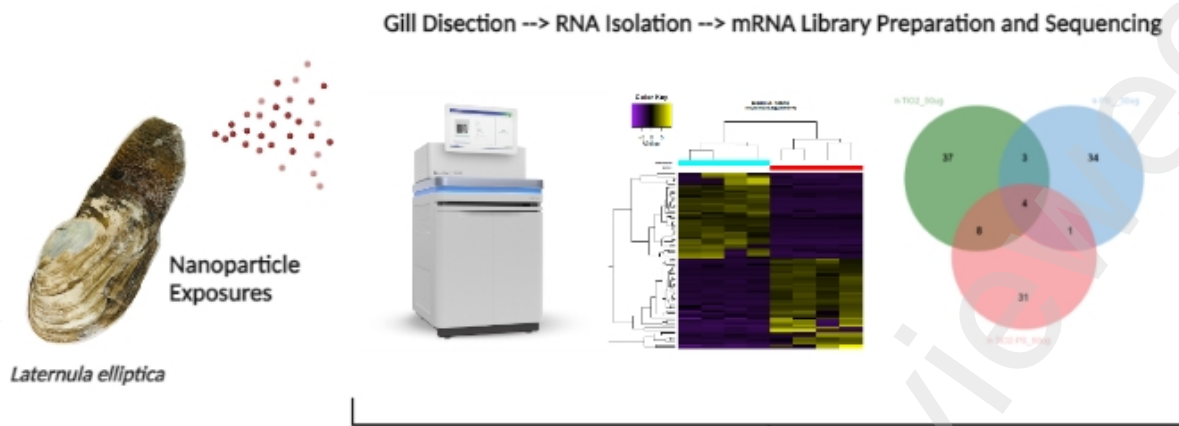
- 28 • Nano-PS-COOH and nano-TiO₂ analyzed with genome-wide gene expression in *L. elliptica*.
- 29 • Gill is a relevant tissue to evaluate toxic effects of nanoparticles in filter-feeders.
- 30 • Exposure to nanoparticles alters relevant molecular functions.
- 31 • Combined nanoparticle exposures produced a particular transcriptional impact.
- 32 • Transcript-target RT-qPCR reveals valuable biomarkers.

34 **Abstract**

35 Contaminants of emerging concern (CEC) have been documented in surface waters, sediment and
36 biota in Southern Ocean. Among CEC, in recent years micro- and nanoplastics and metal-oxide
37 nanomaterials have been found in several environmental compartments. Ecotoxicological
38 consequences to their exposure are almost unknown for Antarctic aquatic species and barely
39 addressed so far. The Antarctic soft clam *Laternula elliptica* is an endemic Antarctic species having
40 a wide distribution in the Southern Ocean. Being a filter-feeder, it could act as suitable bioindicator
41 of pollution from CEC also considering its sensitivity to various sources of stress. The present study
42 aims to assess the impact of polystyrene nanoparticles (PS NP) and the nanometal titanium-dioxide
43 (n-TiO₂) on genome-wide transcript expression of *L. elliptica* either alone and in combination and at
44 two toxicological relevant concentrations (5 and 50 µg/ml). Transcript-target q-RT-PCR was
45 performed with the aim to identify suitable biomarkers of exposure and effects. The experimental
46 exposures showed gene expression profiles with the control group always clustered together (at both
47 concentrations), however, as expected at the highest concentration the clustering was clearer between
48 control and exposed clams. A total of 221 genes resulted differentially expressed in exposed clams
49 and control ones, and 21 of them had functional annotation such as ribosomal proteins, antioxidant,
50 ion transport (osmoregulation), acid-base balance, immunity, lipid metabolism, cell adhesion,
51 cytoskeleton, apoptosis, chromatin condensation and cell signaling. Although few transcripts were
52 shared as differentially expressed between the experimental treatments compared to control, At
53 function level relevant ones were shared among some treatments and could be considered as general
54 stress due to nanoparticle exposure. After applying transcript-target approach duplicating the number
55 of clam samples, four ecologically relevant transcripts were revealed as biomarkers for nanoplastics,
56 n-TiO₂ and their combination at 50 µg/ml, that could be used for monitoring clams' health status in
57 different Antarctic localities.

58

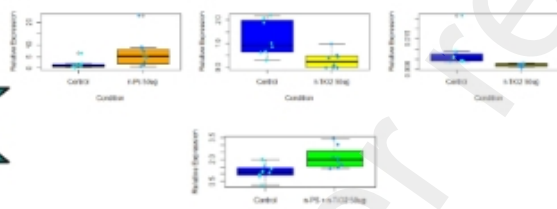
59 Abstract figure



Future Antarctic population health Status



q-RT-PCR --> Molecular Biomarkers revealed



60

61 Keywords

62 Nanoplastic, nanometal, toxicity, Gene expression, biomarkers

63 **1 Introduction**

64 The Antarctic continent and surrounding waters are currently protected by international laws of the
65 Antarctic Treaty and since the late 90s, the Committee for Environmental Protection (CEP) has
66 increased the efforts to develop management tools for environmental impact assessment, monitoring
67 and marine pollution. Despite such efforts, Antarctica is currently under threat from increasing
68 anthropogenic pressures. Recent studies have revealed various contaminants of emerging concern
69 (CEC) in Southern Ocean ecosystems. Among CECs observed in Antarctic waters, pharmaceuticals
70 and personal care products have been detected in seawaters around King George Island (Perfetti-
71 Bolaño, A. et al., 2022; Szopińska et al., 2022). Furthermore, 54 CECs have been linked to human
72 presence in the Northern Antarctic Peninsula, and thus potentially increasing environmental risk by
73 affecting marine life and ecosystems (Olalla et al. 2020). Concerning persistent halogenated organic
74 CECs, hexachlorobenzene (HCB), BDE-209, heptachlor, oxychlorane and mirex have been the main
75 pollutant recorded in tissues of marine benthic invertebrates at Rothera Point in the Antarctic
76 Peninsula (Cunha da Silva et al., 2023; Krasnobaev et al., 2020). The ever-increasing amount of
77 plastic litter found in Southern Ocean is the most probable source of CEC pollution, originating both
78 from research stations and fishing operations, but also from transport by ocean currents, and wind-
79 generated water movements (Caruso et al., 2022; Rota et al., 2022).

80

81 A number of studies have shown that plastic pollutants as macro- (>10mm) and meso-sized (1-10
82 mm) plastics are present in the Southern Ocean waters (Lacerda et al., 2019; Suaria et al., 2020), as
83 well as microplastic (Isobe et al., 2017; Lacerda et al., 2019; Waller et al., 2017). The origin of micro-
84 (1-1000 μm) and nanoplastics (<1 μm) is not yet determined, however Leistenschneider et al. (2021)
85 showed that 45% of microplastic collected in the Weddell Sea derived from vessel-induced
86 contamination. On the other hand, the hypothesis of transport by Antarctic base effluents and currents
87 from other oceans should not be excluded. Further evidence of microplastics in Antarctica is
88 represented by recent records in sediments of the Ross Sea (Munari et al., 2017) and Antarctic sea ice
89 (Kelly et al., 2020), revealing the availability of these CEC for the trophic web, including organisms
90 as the Antarctic krill. Dawson et al (2018) demonstrated that Antarctic krill can digest microplastic
91 particles into nanoplastics, enhancing the transfer of such pollutants along trophic webs. Besides,
92 nanoplastic debris has been recorded in Antarctic sea ice with 52.3 ng/ml average concentration,
93 demonstrating that the occurrence of plastic at nanosized scale in Antarctic ice and water is now real
94 (Materić et al., 2022). In terms of ecotoxicological risks for Antarctic marine life, invertebrates, such
95 as filter-feeders and bottom grazers, are probably the most exposed to the fraction of plastic litter
96 accumulating in sediments, as shown by microplastics found in specimens from the Ross Sea
97 (Bergami et al., 2023; Sfriso et al., 2020).

99 Differently, metal-oxides nanoparticles belonging to CEC have been barely investigated in Antarctic
100 marine species. Their presence has yet to be demonstrated in Antarctic ice and waters, but they are
101 likely to be present as a result of the increasing activities of scientific stations, tourism, and fishery.
102 In other latitudes, as temperate areas, the most commercially common titanium dioxide in the
103 nanoscale form (n-TiO₂) has been detected at concentrations ranging from 20 to 900 µg/L in
104 Mediterranean surface waters (Labille et al., 2020). Sunscreen and cosmetic products, as well as post-
105 consumer material are likely to deliver metal-oxide nanomaterials into marine coastal waters (Haynes
106 et al., 2017). We anticipate that the presence of nanoscale material in the Southern Ocean is highly
107 possible, reaching this region by transport from other oceans and by human activities in Antarctica.
108 Their toxicity toward benthic filter-feeding occupying an important level in the trophic network
109 definitely deserves further exploration. The effect of nanoplastics and metal-oxide nanomaterials
110 should be considered in marine Antarctic biota as previously performed in other regions of the world
111 (Trevisan et al., 2022). Furthermore, the combined potential synergistic effects deserve to be explored
112 in marine Antarctic metazoans, playing a significant ecological role in the marine trophic webs (Das
113 et al., 2022). It is suggested that Antarctic filter-feeding mollusks are among the most sensitive marine
114 metazoans (Peck, 2018), hence species such as *Laternula elliptica* could be considered as target in
115 some areas of the Antarctic coast (Lister et al., 2015). Besides, this species has already been proposed
116 as a suitable sentinel of anthropogenic pollution in Antarctic marine coastal areas, as marine bivalves
117 in others regions of the world (Li et al., 2019). Gills and digestive glands are the most affected target
118 organs by CEC exposure, with histopathological alterations and inflammatory response observed
119 (Jeyavani et al., 2022; Teng et al., 2021). Gills in particular play an essential role in feeding and
120 respiration as first barrier with the external environment, thus more exposed to nanoplastics and
121 metal-oxide nanomaterials present in seawater (Shao et al., 2021; Zhou et al., 2022).

122

123 Transcriptomic is an approach which has been previously applied to pollution monitoring and effect
124 assessment (Blalock et al., 2018), particularly performing experimental designs with control and
125 treatment conditions to be compared. The potential for using RNA sequencing (RNA-seq) to study
126 complex responses of non-model organisms to environmental pressure is evident in a rapidly growing
127 body of literature (Oomen and Hutchings, 2017). The high dimensionality of transcriptomic responses
128 enables their usage as highly specific fingerprints of exposure, and these fingerprints can be used to
129 diagnose environmental stress (Reid and Whitehead, 2016). In addition, molecular biomarkers can be
130 revealed with this approach, for example, Förlin et al. (2019) identified potential transcriptomic
131 biomarkers of toxic compounds in Baltic perch, and similar analysis produced biomarkers in
132 gastropods exposed to Cadmium (Gu et al., 2019). In contrast to other model organisms few studies

133 have examined the impact of CEC in marine bivalves at the transcriptome level. Transcriptomic
134 analysis can not only screen the ecotoxicity of CEC but also infer the function and specific regulatory
135 mechanism of the corresponding unknown genes. As far as bivalve species from temperate areas such
136 as Manila clam, Milan et al. (2013) obtained 162 transcripts correlated with at least one kind of
137 pollutant found in the studied area, of which seven were assigned as correct biomarkers in the most
138 polluted location. Gardon et al. (2020) demonstrated a set of dose-specific transcriptional biomarkers
139 in oysters exposed to microplastics involved in detoxification process, oxidative stress damage and
140 immunity.

141
142 Transcriptional response to different stressors has been previously addressed in the Antarctic soft
143 clam *L. elliptica*, including responses to shell damage (Clark et al., 2010; Sleight et al., 2015), injury
144 and starvation (Husmann et al., 2014), and thermal stress (Truebano et al., 2010). This clearly
145 validated *L. elliptica* as a good indicator for stress exposure, making this mollusk an ideal candidate
146 to be a sentinel species in the Southern Ocean. Nevertheless, responses to CEC exposure have not yet
147 to be addressed in this species. We anticipate that model nanoplastics such as polystyrene
148 nanoparticles (PS NP) and n-TiO₂ exposures may provoke sub-lethal gene expression alterations,
149 affecting some eco-physiological functions. The aim of this work was to study the transcriptomics
150 response to CEC (PS NP and n-TiO₂) exposure in gill tissue of *L. elliptica*, expanding the analysis to
151 identify biomarkers of nano-pollutants. Accordingly, we applied a whole genome-wide
152 transcriptomic analysis (RNAseq) to unravel differentially expressed transcripts of relevant molecular
153 functions for each contaminant and synergic effect of co-exposure at two concentrations (5 and 50
154 µg/mL). Then, a transcript-target RT-qPCR analysis was applied on double the number of organisms
155 (n = 8) to validate biomarkers that could be used *in situ*.

156

157 **2 Methods**

158 Sampling Antarctic soft clams: a total of 120 *Laternula elliptica* adult (average shell length of
159 71.66±11.75 cm, mean ± standard deviation, SD) was collected by SCUBA diving in Fildes Bay,
160 King George Island (South Shetland Islands), in January 2020 (Figure 1).

161

162 2.1 Preparation of nanoparticles suspension for experimental exposure:

163 Carboxyl-modified PS NP (PS-COOH NP), with a nominal size of 62 nm, were purchased from
164 Bangs Laboratories Inc. (catalog code: PC02N, suspension at 10.1%), while n-TiO₂ was kindly
165 provided by Degussa Evonik as Aeroxide® P25 (powder composed of 82–18% anatase - rutile crystal
166 structure) with a nominal size of 25 nm. From the PS-COOH NP stock suspension, an intermediate
167 suspension was prepared in MilliQ water at the concentration of 10 mg/mL and 250 and 25 µg/mL),

168 sonicating the suspensions using the bath sonicator DENTSPLY Ultrasonik 57H for 2 min (Murano
169 et al., 2021) and vortexed prior to use as described by (Bergami et al., 2020). Two working
170 suspensions at 250 and 25 $\mu\text{g}/\text{mL}$ were then prepared and 1 mL of each suspension was added to 5 L
171 tanks of natural sea water (NSW) to achieve final concentrations of 50 and 5 $\mu\text{g}/\text{mL}$, respectively.

172

173 As for n-TiO₂, a stock suspension (10 mg/mL) was prepared in MilliQ water, vortexed and sonicated
174 for 1 hour, always keeping the suspension in cold water (changing water each ~ 10 min) (Della Torre
175 et al., 2015). Two intermediate suspensions were then prepared at 250 and 25 $\mu\text{g}/\text{mL}$, and 1 mL of
176 each was added to 5 L tanks containing NSW to reach concentrations of 50 and 5 $\mu\text{g}/\text{mL}$, respectively.
177 Tested suspensions were replaced every 24h for a semi-static *in vivo* exposure. The NSW used for
178 the experiments (temperature of $0\pm 1^\circ\text{C}$, pH of 8.42 and salinity of 32.8‰) was taken from Fildes
179 Bay where the specimens were also collected.

180

181 Secondary characterization of PS-COOH NP (at 50 $\mu\text{g}/\text{mL}$, following Bergami et al., 2019, 2020)
182 and n-TiO₂ (at 5 $\mu\text{g}/\text{mL}$, based on Della Torre et al., 2015) in NSW was carried out by Dynamic Light
183 Scattering and electrophoretic mobility. For this purpose, NSW was first filtered at 0.20 μm to allow
184 the removal of large suspended natural colloids that would interfere with the analysis. Nanoparticle
185 size-related parameters (e.g., Z-average, expressed in nm) and surface charge (ζ -potential, expressed
186 in mV) resulted from 3 independent measurements and were obtained at 0°C (Z-average) and 4°C (ζ -
187 potential).

188

189 2.2 Experimental design: After 2 days of acclimation of the specimens in NSW, two independent
190 experiments (96h) were carried out. Individuals ($n = 5$) were placed in 5L tanks with the following
191 test solutions: NSW only (control), PS-COOH NP at 5 and 50 $\mu\text{g}/\text{mL}$, n-TiO₂ at 5 and 50 $\mu\text{g}/\text{mL}$ and
192 combined exposure (PS-COOH NP and n-TiO₂) at 5 and 50 $\mu\text{g}/\text{mL}$. Tanks were permanently well
193 oxygenated and specimens exposed with a photoperiod of 18/6 light/obscurity intervals. After 96h,
194 clams were dissected for tissue extractions (gills), frozen with liquid nitrogen, put in 1ml of RNAlater
195 and kept at -80°C .

196

197 2.3 RNA isolation, library preparation and Illumina NovaSeq sequencing: Eight gill tissues for each
198 treatment, between 15-30 mg, were weighed on an analytical balance, and RNA isolated using
199 E.Z.N.A.® Total RNA Kit I (Omega Bio-Tek), following the protocol instructions. The RNA
200 concentrations of each sample were measured with Tecan infinite m200 pro spectrophotometer. Four
201 sample replicates by conditions ($nt = 32$) were used for library preparation (with TrueSeq Stranded

202 mRNA Kit; Illumina) and Illumina NovaSeq sequencing in DNALink Company (San Diego, United
203 States).

204

205 2.4 Bioinformatic analyses: 32 paired-end libraries were obtained from Illumina NovaSeq 6000
206 sequencing (four biological samples by conditions). The raw sequences were analyzed under Galaxy
207 Platform ABIMS from Station Biologique de Roscoff (<https://galaxy.sb-roscoff.fr/>) and from Institut
208 Française de Bio-informatique (<https://usegalaxy.fr>), until finding the differentially expressed
209 transcripts between controls and treatments. Firstly, the raw sequences were checked for quality,
210 using a phred score > 30 as criteria. The 9 first nucleotides and last one did not pass this criterion. For
211 these reasons, the first 9 nucleotides and the last one of all raw reads were trimmed with “Trim
212 sequences” program Galaxy Version 1.0.2 (Gordon 2010). Then, a reference transcriptome was
213 assembled using all libraries with Trinity (Grabherr et al., 2011), followed by ortholog regrouping to
214 reduce functional redundancy using with CDHit (Fu et al., 2012) and the final transcripts were
215 annotated with the Trinotate workflow. Completeness and redundancy degree were assessed with
216 BUSCO software (Simão et al., 2015). Salmon was used to count reads using the assembled reference
217 transcriptome as input, with the relative orientation of reads within a pair “Inward”, strandedness “U”
218 (not stranded) and type of index “quasi” (Patro et al., 2017). The TPM normalized counts were used
219 to generate expressions matrixes matrices of transcript expression among experimental conditions.
220 Then, these matrixes were used to obtain the differentially expressed genes (DEG) at isoform level
221 using DEseq2 software (Love et al., 2014), considering DEG with a $\log_2(\text{foldchange}) > 1.5$ (fold-
222 change>3) and False discovery rate < 0.05.

223

224 2.5 qRT-PCR amplification: cDNAs were synthesized from RNA samples, using M.MLV reverse
225 transcriptase, reaction buffer RNases-free, oligo(dt)₂₀, random hexamers, RNaseOUT™
226 Recombinant Ribonuclease Inhibitor and dNTP (all these reagents from Thermo-Fisher Invitrogen®),
227 following protocol instructions and using conventional thermocycler SimpliAmp (Applied
228 Biosystems). The amplification reaction cycles were performed according to manufacturer’s
229 instructions. The qPCRs primers were designed for all differentially expressed transcripts with
230 functional annotation and the reference transcripts, using “Expasy translate”
231 (<https://www.expasy.org/>) software to verify 5’→3’ sense and “Amplifx” to find the best primers for
232 each sequence. The primer design criteria were: 1) a length between 18-24 bp, 2) with a melting
233 temperature difference no higher than 1°C, 3) qPCR product length between 90 and 200 bp, 4) GC
234 percent superior to 45%. The “oligo Calc” software
235 (<http://biotools.nubic.northwestern.edu/OligoCalc.html>) was used to assess the melting temperature
236 and confirm that no fork nor dimer formation occurs. Primer sequences are given in table

237 1(Supplementary File 1). A conventional gradient PCR was performed for each pair of primers
238 designed with 200 nM concentration, from 54.8 to 64.6, to determine the optimal temperature. The
239 PCR program was: 1) hot start at 95°C for 10 minutes; 2) 40 cycles with 95°C for 30 seconds, the
240 temperature gradients for 1 minute, and finalize with 72°C for 30 seconds. Then, the melting curve
241 was produced with real-time thermocycler AriaMx (Agilent) to choose the best unique peak (taking
242 the highest). The melting curve program was (0.5 °C of resolution): 1) 95°C for 1 minute; 2) 30
243 seconds at 55°C and 3) 30 seconds at 95°C. After this, an electrophoresis in agarose gel (1.7%) was
244 performed to ensure that only one transcript is amplified. Once the primers were validated at the best
245 temperature, a Q-RT-PCR was performed with eight samples by conditions, With the Brilliant II
246 SYBR® Green QPCR Master Mix, following product protocol instructions. Finally, relative
247 expressions for eight samples per condition of each transcript were calculated following the $2^{-\Delta\Delta C_t}$ of
248 Livak and schmittgen (2001), normalized with the reference transcripts “NADH deshydrogenase
249 (Ubiquinone) 1 subunit beta subcomplex 8”, recorded as stably expressed with RNAseq data. This
250 taking into account a ratio between TPM average for all 32 samples and Standard Deviation, in order
251 to choose the least variable with a high gene expression level in our RNAs samples.

252

253 2.6 Statistical analyses: Shapiro test and Bartlett test were performed to assess the normal distribution
254 and homoscedasticity respectively using Rstudio scripts. According to these results t-test (parametric)
255 or Mann-Whitney (non-parametric) were performed between the relative expression of control and
256 treatment condition using GraphPad Prism 5, considering a 95% of confidence (p-value < 0.05).

257

258 2.7 Data availability: Raw Illumina NovaSeq 6000 paired-end reads are available in the NCBI
259 BioProject PRJNA962035 (<http://www.ncbi.nlm.nih.gov/bioproject/962035>).

260

261 **3 Results and Discussion**

262 The characterization analysis confirmed the agglomeration behaviour of n-TiO₂ in high ionic strength
263 media, with an average hydrodynamic size of 872.9 ± 73.8 nm in NSW and a weak negatively surface
264 charge (-11.7 ± 0.7 mV). We previously reported instability and large agglomeration of n-TiO₂ (25
265 nm, anatase, from Sigma-Aldrich) in Antarctic rock pool waters (González-aravena et al., 2022) and
266 our results are in line with previous studies in seawaters for this NP (reviewed in Corsi et al., 2020,
267 2021). For example, Della Torre et al. (2015) reported the formation of micrometric agglomerates
268 (~970 nm) in artificial sea water for the same n-TiO₂ (Aeroxide® P25) at 10 µg/mL. Similarly, as far
269 as PS-COOH NP, a large agglomeration (average size of 752.7 ± 137 nm) and a negative surface
270 charge (-25.2 ± 1.8 mV) were observed in Antarctic NSW. Size-related parameters largely differ from
271 our previous findings for this NP in seawater collected from the same coastal area (Bergami et al.,

272 2019), in which we showed only slight initial agglomeration (173 ± 21 nm) compared to NP nominal
273 size (50 nm). Such difference could be attributed to the different batch of NP used (Bangs
274 Laboratories Inc. in the present study vs Invitrogen in Bergami et al., 2019) or to the different
275 composition/abundance of natural colloids present in the NSW. Our results highlight the need to apply
276 characterization analysis on a case-by-case study in nano-ecotoxicological studies (Corsi et al., 2021,
277 2020).

278

279 The present genome-wide transcriptomic (RNAseq) analysis yielded 975,727,394 paired-end reads
280 from 32 *L. elliptica* gills (four samples by experimental condition), having a high-quality data with
281 an average nucleotide phred score of 36.11 and average of percent bases over 30 phred score of
282 94.75%. After trinity assembly and CD-Hit orthologs grouping an exhaustive Transcriptome was
283 constructed with 251,294 Transcripts for the 32 clam individuals with a N50 of 955 bp. A functional
284 transcriptome assessment was performed with BUSCO reporting a high completeness for metazoan
285 transcriptomes (99.4%) and low duplication rate (7.0%), having 92.4 single transcripts, only 0.6% is
286 fragmented and no transcripts missing (0%) (Table 1). Among the 251,294 transcripts, a potential
287 annotation could be attributed to 26,324 (10.48%) using the trinotate workflow. After filtering
288 transcripts with an expression level below 10.00 and isoforms below 10% of representation, the
289 annotation rate increased to 19.72%.

290

291 Results from experimental exposure showed the gene expression profiles at the lowest concentration
292 tested of 5 $\mu\text{g/ml}$ are shown in (Figure 2), with control samples clustered apart and only two
293 individuals exposed to PS-COOH NP clustered closer to the control group than with the other 2
294 individuals of the same condition. On the contrary, specimens exposed to n-TiO₂ clustered together
295 while the co-exposed ones were not clearly separated even though they still belonged to the clusters
296 of exposed ones. Similarly, at the highest tested concentration of 50 $\mu\text{g/ml}$, control group clustered
297 separately, but without treatment samples in this case (Figure 3). The findings of the clustering
298 analysis suggest that a concentration-dependent gene expression profile could be hypothesized for
299 both nanoparticles tested irrespective of the size and core composition (62 vs 25 nm, PS-COOH NP
300 vs n-TiO₂).

301

302 This global transcriptomic analysis recorded 25, 56 and 43 DEG for PS-COOH NP, n-TiO₂ alone and
303 in combination for the 5 $\mu\text{g/ml}$ in comparison with control condition (supplementary file 2).
304 Regarding the highest concentration tested of 50 $\mu\text{g/ml}$, 43, 53 and 45 DEG were detected for PS-
305 COOH NP, n-TiO₂ and their combination in comparison to controls (supplementary file 2). The Venn
306 diagram analysis shows a low overlap considering all DEG of each treatment at 5 and 50 $\mu\text{g/ml}$, with

307 only 1 DEG shared among single and combined exposure conditions at 5 $\mu\text{g}/\text{ml}$ (Figure 4A) and 4
308 DEG at 50 $\mu\text{g}/\text{ml}$, (Figures 4B). Furthermore, these diagrams also reveal few shared DEG between
309 pairs of treatments, with from 2 to 5 shared DEG at 5 $\mu\text{g}/\text{ml}$, and from 1 to 8 shared DEG at 50 $\mu\text{g}/\text{ml}$.
310 Within a same treatment, no shared DEG between the two concentrations of PS-COOH NP were
311 found, while five DEG were shared between the two concentrations of n-TiO₂ and one shared DEG
312 when combined (Figure 4C-E). A more pronounced effect of nanoparticles exposure at higher
313 concentration was found (Figure 4 A and B), with more shared DEG, also suggesting the
314 concentration-dependent effect on gill transcriptome of *L. elliptica*. Gardon et al. (2020) reported a
315 similar concentration-dependent transcriptomic effect of micro-PS exposure at three concentrations
316 (0.25, 2.5, and 25 $\mu\text{g}/\text{L}$), with different responses recorded mainly for antioxidant and immune genes.
317
318 Our differential analysis allowed us to identify a total of 221 genes which were differentially
319 expressed when comparing nanoparticles with control conditions. Among them, 21 have been
320 attributed to a potential function after the annotation with the trinotate workflow (supplementary file
321 3, Table 1). Interestingly, the annotation of these different genes converges toward some similar
322 functions depending on the treatment and the concentration tested. Notably, functions related to
323 structural constituent of ribosome, ions and particles transport, cell signaling, oxidative stress and
324 immunity are affected in response to nanoparticles exposure regardless of size and core composition.
325 The expressions of genes coding for ribosomal proteins were altered in response to both nanoparticles.
326 A transcript (TRINITY_DN101707_c0_g1_i13) encoding for a “60S ribosomal protein L7”, is up-
327 regulated by 6.96 and 7.07 log₂ Fold-change in response to PS-COOH NP and both nanoparticles
328 exposure at 5 $\mu\text{g}/\text{ml}$ respectively (table 2 and sup file 2). This is in line with a previous study on the
329 marine rotifer *Brachionus koreanus*, where Ribonucleoprotein Complex Biogenesis genes were
330 differentially expressed in response to single exposure to non-functionalized PS NP of 50 nm at 1
331 $\mu\text{g}/\text{ml}$ (Jeong et al., 2021). Furthermore, the expression of the gene (for transcript:
332 TRINITY_DN127464_c0_g2_i14) encoding for a 60S ribosomal protein L23 was repressed by -2.74
333 and -3.49 log₂Fold-Change respectively, in response to n-TiO₂ exposure and to both nanoparticles at
334 50 $\mu\text{g}/\text{ml}$ (table 2 and sup file 2). The effects of silver NP on the expression of genes encoding for
335 ribosomal proteins has previously been reported in *Danio rerio* embryos (Van Aerle et al., 2013), and
336 in different developmental stages of *Chironomus riparius* (Nair et al., 2011). Altogether, our analyses
337 are in line with previous works and they indicate that the expression of genes encoding for structural
338 constituent of ribosome is sensitive to nanoparticles exposure, even at low concentration; this may
339 result in dysregulation in ribosome protein configuration. Another shared molecular function altered
340 in response to both nanoparticles exposure was related to “ion transport gene Solute Carrier family
341 23”. The expression of two genes (for transcripts TRINITY_DN246_c2_g2_i1 and

342 TRINITY_DN3151_c0_g1_i1) encoding for Solute carrier family 23 members were up regulated in
343 response to n-TiO₂ alone and in combination at 5 µg/ml (7.044 log₂Fold-Change) at both
344 concentrations tested (5 µg/ml and 50 µg/ml) (6.79 log₂Fold-Change and 1.91 log₂Fold-Change
345 respectively) (Table 2 and sup file 2). Considering that these genes are potentially involved in ion
346 transport (Zhang et al., 2017), it could be expected that the osmoregulation process might be affected
347 in response to nanoparticles exposure in gills of *L. elliptica*. Furthermore, this situation is
348 accompanied by down-regulation of the expression of vesicular traffic gene (Ap-4 Complex
349 accessory subunit tepsin, transcript id: TRINITY_DN24516_c0_g1_i10), upon n-TiO₂ exposure to 5
350 µg/ml with -2.29 log₂Fold-Change, as described in zebrafish embryos (Jovanovic et al., 2011). This
351 study showed that cell membrane transporter and vesicle transport transcripts were down-regulated
352 in response to carbon-based nanoparticles (hydroxylated fullerenes at 40 µg/ml), suggesting NP
353 interference in recycling process of vesicular organelles. Also, at the higher dose of n-TiO₂ (50
354 µg/ml), we observed a down-regulation of cytoskeleton function transcript Tubulin alpha-3 chain
355 (TRINITY_DN82866_c4_g1_i1) with -5.75 log₂FoldChange. Similar results were recorded in
356 mollusks such as the bivalve *Mytilus galloprovincialis* with up-regulation of the expression of gene
357 encoding for cytoskeletal transcript in digestive gland after n-TiO₂ exposure (Banni et al., 2016). Also
358 in gilthead sea bream *Sparus aurata* down-regulation of the expression of gene encoding for Alpha-
359 actinin 1 was observed in liver in response to citrate coated gold NP of ~40 nm diameter at 50 µg/ml
360 (Teles et al., 2019). Altogether, our work indicates convergent molecular patterns in response to
361 nanoparticles exposure, revealing how which gill cell uptake and transport of ions and particles are
362 affected by nanoparticles exposure.

363

364 Other molecular functions affected in response to nanoparticles and shared between the two exposures
365 were related to oxidative stress and immunity. The expression of genes encoding for antioxidant
366 functions were up-regulated: “TRINITY_DN4299_c0_g1_i16” encodes for a putative ferric-chelate
367 reductase 1 and “TRINITY_DN6514_c1_g1_i6” encodes for glutathione S-transferase omega-like 2;
368 the expression of both these genes is upregulated by 2.17 and 3.35 log₂FoldChange respectively in
369 response to PS-COOH NP at 50 µg/ml (table 2 and sup file 2). “TRINITY_DN3207_c5_g2_i2”
370 transcript encodes for DBH-like monooxygenase protein 1 and “TRINITY_DN5798_c1_g1_i1”
371 encodes for a putative Thioredoxin, which plays a key role in cell protection from the detrimental
372 effects of reactive oxygen species (Lee et al., 2013). The expression of these two genes is up-regulated
373 by 1.98 and 22.78 log₂FoldChange respectively in response to combined exposure to PS-COOH NP
374 and n-TiO₂ at 50 µg/ml (table 2 and sup file 2). This up-regulation of the expression of oxidative
375 stress responsive genes is concordant with previous studies that observed antioxidant transcripts
376 dysregulation in marine invertebrates, such as in the mussel *Mytilus spp.* in response to PS NP (Paul-

377 Pont et al., 2016). Antioxidant and xenobiotic responses have been described upon exposure to PS
378 NP, such as the up-regulation of glutathione S-transferase, in aquatic invertebrates like *Daphnia pulex*
379 (Liu et al., 2021), and the crayfish *Cherax quadricarinatus* (Cheng et al., 2022). Interestingly,
380 translation and antioxidant transcript expression has been altered at 5 and 50 µg/ml respectively,
381 similar to what was reported for the swamp crayfish, *Procambarus clarki*, upon PS NP orally
382 administered (Capanni et al., 2021).

383

384 Regarding immune transcripts, we also recorded the downregulation of expression of a gene
385 (TRINITY_DN7242_c3_g1_i1) annotated as Deleted in malignant brain tumors 1 protein (DMBT1),
386 differentially expressed in response to n-TiO₂ at 50 µg/ml with -2.63 log₂Fold-Change (table 2 and
387 sup file 2). This gene encodes for a member of scavenger receptor cysteine rich (SRCR) protein
388 family and has possible functions in innate immunity, inflammation and epithelial cell differentiation
389 (Madsen et al., 2010). Effect on immune response genes has been reported in zebrafish gill tissues in
390 response to Fe₃O₄ NP exposure (Zheng et al., 2018). “TRINITY_DN7095_c0_g1_i22” is annotated
391 as a transcript encoding for Tachylectin-5A and its expression is repressed by -1.95 log₂Fold-Change
392 in response to both nanoparticle exposure at 50 µg/ml. Tachylectins are pattern recognition molecules
393 with a key role in the innate immune system, known to be involved in specific recognition of invading
394 microbes through acetyl group-containing molecules (Angthong et al., 2017).

395

396 Another transcript potentially involved a lipase gene (TRINITY_DN4893_c0_g1_i22), which was
397 significantly up-regulated in n-TiO₂-exposed clams and in those from the combined exposure group
398 at 50 µg/ml with 3.67 and 4.01 log₂Fold-Change respectively. This was the HRSL1 transcript,
399 potentially involved in phospholipase metabolization as glycerophospholipids (Mardian et al., 2015).
400 Membrane glycerophospholipids are known to affect not only the production of lipid mediators but
401 also membrane properties, which could be affected during these exposures and compromise cell
402 membrane permeability in gill tissues.

403

404 The alterations in eco-physiologically relevant gene functions as those observed in the present study
405 upon single and combined exposure to PS-COOH NP and n-TiO₂ are source of concern. The down-
406 regulation of immune genes and the up-regulation of antioxidant responses reveal potential
407 detrimental consequences of ability of clam's gill cells to cope with waterborne nanoparticles
408 exposure. Indeed, such responses at gene level suggest that eco-physiological relevant functions of
409 the Antarctic clams could be compromised from nanoplastics and metal-oxide NP exposure.

410

411 Functions related to cell signaling were also affected in response to NP exposure. The expression of
412 both genes “TRINITY_DN5301_c0_g1_i14” and “TRINITY_DN13854_c0_g1_i4” annotated as
413 “alpha-protein kinase vwka” and “CUB and sushi domain-containing protein 3”, respectively, were
414 induced in response to n-TiO₂, at 5 µg/ml (6.84 and 4.84 log₂Fold-Change up-regulation,
415 respectively). The first one is a cell signaling transcript potentially implicated in a large variety of
416 cellular processes such as protein translation, Mg²⁺ homeostasis, intracellular transport, cell
417 migration, adhesion, and proliferation (Middelbeek et al., 2010). The second one is putatively
418 involved in protein-protein interaction between extracellular and transmembrane proteins. At 50
419 µg/ml n-TiO₂ exposure, the expression of the gene “TRINITY_DN1668_c0_g1_i4” potentially
420 encoding for a serine/threonine-protein kinase roco5 was down-regulated by 4.93 log₂Fold-Change.
421 This transcript belongs to Roco protein family that is characterized by having, among others, diverse
422 regulatory and protein-protein interaction domains, potentially involved in cell division, chemotaxis,
423 and development (Marín et al., 2008).

424

425 In accordance to previously published studies, our analysis also highlighted that the expression of the
426 gene “TRINITY_DN2086_c1_g1_i14” which potentially encodes for caspase 8 is down-regulated by
427 5.17 log₂Fold-Changes in response to n-TiO₂ at the highest exposure concentration of 50 µg/ml
428 (shown in Table 2 and sup file 3). A differential expression of genes involved in the apoptotic pathway
429 in response to NP has been previously reported in zebrafish embryos exposed to Cu/TiO₂ and TiO₂
430 (Yeo and Park, 2012). Similarly, a set of apoptosis genes resulted differentially expressed in the
431 digestive glands of the freshwater benthic clam *Corbicula fluminea* probably by oxidative stress
432 induced by PS NP in this case (Li et al., 2021). Also, different concentrations of silicon dioxide and
433 copper oxide NP affected Caspase3 gene expression in gill and liver of *Oreochromis niloticus* fish
434 (Abdel-latif et al., 2021). The transcript “TRINITY_DN88636_c0_g1_i7” encodes a putative
435 “Barrier to Autointegration Factor” with function related to chromatin condensation for multiple
436 pathways including mitosis, post-mitotic nuclear assembly, intrinsic immunity against foreign DNA,
437 transcription regulation, and the DNA damage response (Sears and Roux, 2020). It is induced by 4.8
438 log₂Fold-Change in response to 50 µg/ml n-TiO₂ exposure (Table 2 and sup file 2). Furthermore, the
439 combined exposure to 5 µg/ml revealed the up-regulation of another gene, coding the Carbonic
440 anhydrase 9 (TRINITY_DN494_c17_g1_i11), which catalyzes the reversible hydration of carbon
441 dioxide in the reaction: CO₂ + H₂O H⁺ + HCO³⁻. This transcript is potentially implicated in several
442 physiological processes, such as acid-base balance, CO₂ and HCO³⁻ transport and respiration (Kallio
443 et al., 2010), being highly relevant in *L. elliptica* gill function and homeostasis. Finally, the significant
444 expression increase in the gene “TRINITY_DN1607_c2_g1_i8” potentially encoding for Sushi von

445 Willebrand factor type A transcript was observed in response to combined exposure to NP at 50 µg/ml
446 with 6.23 log₂Fold-Change, being potentially implicated in cell adhesion (Glait-santar et al., 2012).
447
448 RNAseq analysis led us to identify DEG that may be relevant transcripts for biomarkers of early NP
449 exposure (96 h) at toxicologically relevant concentrations (Al-sid-cheikh et al., 2018; Sun et al.,
450 2016). We first found a statistically significant correlation (**p-value = 0.0416, Spearman rank**
451 **correlation rho = 0.428**) of log₂ qRT-PCR Fold-Change against log₂ RNAseq Fold-Change with all
452 transcripts (of 5 and 50 µg/ml DEG detected) (supplementary file 3, Figure 1). We then performed a
453 target transcript q-RT-PCR using eight *L. elliptica* samples in 19 relevant genes (Supplementary File
454 3, Figures 2-4). Interestingly, at the 5 µg/ml exposure, a tendency was observed toward the same
455 results in qPCR as for the RNA-seq analysis for some candidate genes (5 genes out of the 8 tested),
456 AP-4 complex accessory subunit tepsin, Solute carrier family 23 member 2 (for two treatments),
457 Alpha-protein kinase vwka and Carbonic anhydrase 9 (supplementary file 3, Table 2) but not to a
458 statistically significant level. This clearly indicates that the consequences of NP exposure at this
459 concentration is mitigated, confirming our previous observation on the clustering of the data at the 5
460 µg/ml. Working with samples obtained after exposure at the highest concentration (50 µg/ml), a
461 tendency toward the same results as for the RNA-seq analysis in 12 genes out of the 15 tested was
462 observed (supplementary file 3, Table 2). The differential expression of four relevant genes at a
463 statistically significant level in the 8 individuals tested was revealed by qPCR. The gene encoding for
464 the transcript “**Glutathione S-transferase omega-like 2**” had significant relative expression
465 difference (p-value = 0.0379) in response to PS-COOH NP exposure (Supplementary File 3, Figure
466 2). This suggests that antioxidant and metabolism of xenobiotic transcript could be suitable biomarker
467 to indicate the presence of relevant concentrations of PS NP. Several studies have showed the use of
468 these transcripts as a biomarker in response to NP exposures in bivalves, but most of them were
469 assessed in response to metal-oxide NP only (Garaud et al., 2016). We suggest here to further use of
470 this Glutathione transcript as a biomarker in response to PS-COOH NP challenge. Furthermore, we
471 found by qPCR that the expression of the gene related to inflammatory process and protection
472 (“**Deleted in malignant brain tumors 1 protein**”) (p-value = 0.0070) was down-regulated in
473 response to n-TiO₂ exposure as for the RNAseq analysis (Supplementary File 3, Figure 3). Transcripts
474 involved in inflammatory immune process have been previously observed as biomarkers of the
475 exposure to diverse nano-metals in aquatic metazoans (Kulasza and Skuza, 2021). We also revealed
476 by qPCR on the 8 individuals the same expression results as for RNAseq for the transcripts annotated
477 as “**Tubulin alpha-3 chain**” (Supplementary File 3, Figure 3) in response to n-TiO₂ exposure (p-
478 value = 0.0007853) and the transcript annotated as “**Solute Carrier Family Member 1**” in response
479 to both nano-pollutants (p-value = 0.0085) (Supplementary File 3, Figure 4). We suggest that these

480 two novel transcripts could be used as valuable novel biomarkers indicating the presence of NP in the
481 environment, including remote regions such as the Southern Ocean.

482

483 Only few studies have performed gene expression analyses in aquatic Antarctic invertebrates
484 following exposure to nanoplastics or nano-metals (Bergami et al., 2022, 2019; González-aravena et
485 al., 2022), however the combined effects more relevant in terms of realistic exposure scenarios have
486 been overlooked (Corsi et al., 2021, 2020). However, no data of genome-wide transcriptomic analyses
487 are yet available for most of polar organisms, including the endemic Antarctic clams *L. elliptica*.
488 Meanwhile, a size-depending effect of nanoplastics have been proposed, with the smaller ones (< 100
489 nm, as those used in the present study) associated with higher toxicity (Hao et al., 2023). Similarly,
490 nano-metals have been reported having a size-depending effect, with those having a low nominal size
491 (e.g., 25 nm in the present study) an highest influx rate in micro-invertebrates such as *Daphnia magna*,
492 and augmenting the possibility of toxic effects (Zhao and Wang, 2012).

493

494 **4 Conclusions**

495 The observed differential expression analysis in gills of *L. elliptica in vivo* exposed to nanoplastics
496 and n-TiO₂ alone and in combination revealed a concentration-dependent effect, which stimulate
497 further studies at concentrations closer to those environmentally relevant in Antarctic coastal waters
498 (e.g., ~50 ng/ml for nanoplastics, as reported in Antarctic sea ice). Exposing *L. elliptica* to 5 µg/ml
499 have clearly impacted clams ecophysiology and related functions but to a lesser extent than at 50
500 µg/ml (Figure 5). The functional annotation of the transcripts clearly revealed that structural
501 constituent of ribosome, ions and particle transport, cell signaling, oxidative stress and immunity, or
502 apoptosis pathway are affected by NP exposure alone and in combination. The observed gene
503 modulation responses were already evident after 96h of exposure, nevertheless, such short exposure
504 time only partially reflects lifelong exposure that Antarctic clams encounter in their natural
505 environment. Applying genome-wide transcriptomic analyses combined with the transcript-target
506 approach using a larger sampling number, valuable ecologically relevant biomarkers were obtained
507 helping to understand how nanoparticles affect molecular functions. These also allowed identifying
508 biomarkers that could be used to monitor clam health status along Antarctic coasts, which are more
509 prone to local anthropogenic pressures. In perspective of this work, it will be necessary to validate
510 the biomarkers on individuals sampled at different Antarctic locations and exposed to different
511 anthropogenic sources of pollution.

512

513 **5 Declaration of competing interest**

514 The authors declare that they have not conflict of interests.

515

516

517 **6 Authors contributions**

518 **Rondon:** Designed experimentations, carried out experimental exposure experiments in Antarctica,
519 performed bioinformatic analyses and wrote the manuscript. **Valdés:** Performed q-RT-PCR,
520 statistical analyses and participated in manuscript drafting. **Cosseau:** Design experimentations,
521 performed transcriptome orthologs clustering analyses (CD-Hit) and participated in manuscript
522 drafting. **Bergami:** Designed experimentations, carried out characterization of nano-pollutant
523 suspensions and participated in manuscript drafting. **Cárdenas:** participated in manuscript drafting.
524 **Balbi:** participated in manuscript drafting. **Pérez-Toledo:** Carried out RNA-extractions, RT-PCR,
525 and participated in q-RT-PCR. **Garrido:** Performed diving sampling in Antarctica and participated
526 in experimental analyses. **Perrois:** carried out experimental exposure experiments in Antarctica.
527 **Chaparro:** Participated in bioinformatics analyses in IHPE Galaxy Platform and participated in
528 manuscript drafting. **Corre:** Participated in bioinformatics analyses in ABIM Galaxy platform. **Corsi:**
529 Designed experimentations, provided nanopollutants and participated in manuscript drafting.
530 **González-Aravena:** Participated in experimentation design and drafting manuscript.

531

532 **7Funding:** This research was funded by the ANID-FONDECYT Grant **Proyecto FONDECYT**
533 **Iniciación N° 11190802.**

534

535 **8 Acknowledgment**

536 We would like to express our gratitude to responsible of bioinformatic platforms Galaxy ABIMS,
537 IFB and IHPE. We are grateful with Centro de Excelencia en Biomedicina en Magallanes (CEBIMA,
538 Universidad de Magallanes), for their support with q-RT-PCR platform. We would like to say thanks
539 to INACH Expeditions department and Alejandro Font, Chief of “Profesor Julio Escudero” Base
540 (King George Island, Antarctica), as well as all logistic personnel of “Profesor Julio Escudero” Base.
541 We also are grateful for the Divers team of IDEAL Center.

542

543 **9 References**

544 Abdel-latif, H.M.R., Shukry, M., Euony, O.I. El, Soliman, M.M., Noreldin, A.E., Ghetas, H.A.,
545 Dawood, M.A.O., Khallaf, M.A., 2021. Functions , Histopathology Characteristics , and
546 Transcriptomic Responses in Nile Tilapia (*Oreochromis niloticus*) Juveniles. *Biology* 10, 183.
547 <https://doi.org/https://doi.org/10.3390/biology10030183>
548 Al-sid-cheikh, M., Rowland, S.J., Stevenson, K., Rouleau, C., Henry, T.B., Thompson, R.C., 2018.
549 Uptake, Whole-Body Distribution, and Depuration of Nanoplastics by the Scallop *Pecten*

550 *maximus* at Environmentally Realistic Concentrations. Environmental Science and Technology
551 52, 14480–14486. <https://doi.org/10.1021/acs.est.8b05266>

552 Anghong, P., Roytrakul, S., Jarayabhand, P., Jiravanichpaisal, P., 2017. Characterization and
553 function of a tachylectin 5-like immune molecule in *Penaeus monodon*. Developmental and
554 Comparative Immunology 76, 120–131. <https://doi.org/10.1016/j.dci.2017.05.023>

555 Banni, M., Sforzini, S., Balbi, T., Corsi, I., Viarengo, A., Canesi, L., 2016. Combined effects of n-
556 TiO₂ and 2,3,7,8-TCDD in *Mytilus galloprovincialis* digestive gland: A transcriptomic and
557 immunohistochemical study. Environmental Research 145, 135–144.
558 <https://doi.org/10.1016/j.envres.2015.12.003>

559 Bergami, E., Ferrari, E., Löder, M.G.J., Birarda, G., Laforsch, C., Vaccari, L., Corsi, I., 2023.
560 Textile microfibers in wild Antarctic whelk *Neobuccinum eatoni* (Smith, 1875) from Terra
561 Nova Bay (Ross Sea, Antarctica). Environmental research 216, 114487.
562 <https://doi.org/https://doi.org/10.1016/j.envres.2022.114487>

563 Bergami, E., Krupinski-Emerenciano, A., Palmeira-Pinto, L., Reina-Joviano, W., Font, A.,
564 Almeida-de Godoy, T., Silva, J.R.M.C., González-Aravena, M., Corsi, I., 2022. Behavioural,
565 physiological and molecular responses of the Antarctic fairy shrimp *Branchinecta gaini*
566 (Daday, 1910) to polystyrene nanoplastics. Nanoimpact 28, 100437.
567 <https://doi.org/https://doi.org/10.1016/j.impact.2022.100437>

568 Bergami, E., Krupinski, A., González-Aravena, M., Cárdena, C.A., Hernández, P., Silva, J.R.M.C.,
569 Corsi, I., 2019. Polystyrene nanoparticles affect the innate immune system of the Antarctic sea
570 urchin *Sterechinus neumayeri*. Polar Biology. [https://doi.org/doi.org/10.1007/s00300-019-](https://doi.org/doi.org/10.1007/s00300-019-02468-6)
571 [02468-6](https://doi.org/doi.org/10.1007/s00300-019-02468-6)

572 Bergami, E., Manno, C., Cappello, S., Vannuccini, M.L., Corsi, I., 2020. Nanoplastics affect
573 moulting and faecal pellet sinking in Antarctic krill (*Euphausia superba*) juveniles.
574 Environment International 143, 105999.
575 <https://doi.org/https://doi.org/10.1016/j.envint.2020.105999>

576 Blalock, B.J., Robinson, W.E., Loguinov, A., Vulpe, C.D., Krick, K.S., Poynton, H.C., 2018.
577 Transcriptomic and Network Analyses Reveal Mechanistic-Based Biomarkers of Endocrine
578 Disruption in the Marine Mussel, *Mytilus edulis*. Environmental Science and Technology 52,
579 9419–9430. <https://doi.org/10.1021/acs.est.8b01604>

580 Capanni, F., Greco, S., Tomasi, N., Giulianini, P.G., Manfrin, C., 2021. Orally administered nano-
581 polystyrene caused vitellogenin alteration and oxidative stress in the red swamp cray fish
582 (*Procambarus clarkii*). Science of the Total Environment 791, 147984.
583 <https://doi.org/10.1016/j.scitotenv.2021.147984>

584 Caruso, G., Bergami, E., Singh, N., Corsi, I., 2022. Plastic occurrence , sources , and impacts in

585 Antarctic environment and biota. *Water Biology and Security* 1, 100034.
586 <https://doi.org/10.1016/j.watbs.2022.100034>

587 Cheng, H., Dai, Y., Ruan, X., Duan, X., Zhang, C., Li, L., Huang, F., Shan, J., Liang, K., Jia, X.,
588 Wang, Q., Zhao, H., 2022. Effects of nanoplastic exposure on the immunity and metabolism of
589 red crayfish (*Cherax quadricarinatus*) based on high-throughput sequencing. *Ecotoxicology*
590 and *Environmental Safety* 245, 114114. <https://doi.org/10.1016/j.ecoenv.2022.114114>

591 Clark, M.S., Thorne, M.A.S., Vieira, F.A., Cardoso, J.C.R., Power, D.M., Peck, L.S., 2010. Insights
592 into shell deposition in the Antarctic bivalve *Laternula elliptica*: Gene discovery in the mantle
593 transcriptome using 454 pyrosequencing. *BMC Genomics* 11, 362.
594 <https://doi.org/10.1186/1471-2164-11-362>

595 Corsi, I., Bellingeri, A., Eliso, M.C., Grassi, G., Liberatori, G., Murano, C., Sturba, L., Vannuccini,
596 M.L., Bergami, E., 2021. Eco-Interactions of Engineered Nanomaterials in the Marine
597 Environment : Towards an Eco-Design Framework. *Nanomaterials* 11, 1903.
598 <https://doi.org/https://doi.org/10.3390/nano11081903>

599 Corsi, I., Bergami, E., Grassi, G., 2020. Behavior and Bio-Interactions of Anthropogenic Particles
600 in Marine Environment for a More Realistic Ecological Risk Assessment. *Frontiers in*
601 *Environmental Science* 8, 60. <https://doi.org/10.3389/fenvs.2020.00060>

602 Cunha da Silva, M., Bergami, E., Gomes, V., Corsi, I., 2023. Occurrence and distribution of legacy
603 and emerging pollutants including plastic debris in Antarctica: Sources , distribution and
604 impact on marine biodiversity. *Marine Pollution Bulletin* 186, 114353.
605 <https://doi.org/10.1016/j.marpolbul.2022.114353>

606 Das, S., Thiagarajan, V., Chandrasekaran, N., Ravindran, B., Mukherjee, A., 2022. Nanoplastics
607 enhance the toxic effects of titanium dioxide nanoparticle in freshwater algae *Scenedesmus*
608 *obliquus*. *Comparative Biochemistry and Physiology Part C: Toxicology & Pharmacology*
609 256, 109305. <https://doi.org/10.1016/j.cbpc.2022.109305>

610 Dawson, A.L., Kawaguchi, S., King, C.K., Townsend, K.A., King, R., Huston, W.M., Bengtson
611 Nash, S.M., 2018. Turning microplastics into nanoplastics through digestive fragmentation by
612 Antarctic krill. *Nature Communications* 9. <https://doi.org/10.1038/s41467-018-03465-9>

613 Della Torre, C., Balbi, T., Grassi, G., Frenzilli, G., Bernardeschi, M., Smerilli, A., Guidi, P., Canesi,
614 L., Nigro, M., Monaci, F., Scarcelli, V., Rocco, L., Focardi, S., Monopoli, M., Corsi, I., 2015.
615 Titanium dioxide nanoparticles modulate the toxicological response to cadmium in the gills of
616 *Mytilus galloprovincialis*. *Journal of Hazardous Materials* 297, 92–100.
617 <https://doi.org/10.1016/j.jhazmat.2015.04.072>

618 Fu, L., Niu, B., Zhu, Z., Wu, S., Li, W., 2012. CD-HIT: Accelerated for clustering the next-
619 generation sequencing data. *Bioinformatics* 28, 3150–3152.

620 <https://doi.org/10.1093/bioinformatics/bts565>

621 Garaud, M., Auffan, M., Devin, S., Felten, V., Pain-devin, S., Proux, O., Rodius, F., Giambérini, L.,
622 Garaud, M., Auffan, M., Devin, S., Felten, V., Pagnout, C., Pain-devin, S., Proux, O., Rodius,
623 F., Sohm, B., Giambérini, L., 2016. Integrated assessment of ceria nanoparticle impacts on the
624 freshwater bivalve *Dreissena polymorpha*. *Nanotoxicology* 10, 935–944.
625 <https://doi.org/10.3109/17435390.2016.1146363>

626 Gardon, T., Morvan, L., Huvet, A., Quillien, V., Soyeux, C., Le Moullac, G., Le Luyer, J., 2020.
627 Microplastics induce dose-specific transcriptomic disruptions in energy metabolism and
628 immunity of the pearl oyster *Pinctada margaritifera*. *Environmental Pollution* 266, 115180.
629 <https://doi.org/10.1016/j.envpol.2020.115180>

630 Glait-santar, C., Pasmanik-chor, M., Benayahu, D., 2012. Expression pattern of SVEP1
631 alternatively-spliced forms. *Gene* 505, 137–145. <https://doi.org/10.1016/j.gene.2012.05.015>

632 González-aravena, M., Iturra, G., Font, A., Cárdenas, C.A., Rondon, R., Bergami, E., Corsi, I.,
633 2022. Unravelling the suitability of *Branchinecta gaini* as a potential biomonitor of
634 contaminants of emerging concern in the Antarctic Peninsula region. *Antarctic Science* 34,
635 281–288. <https://doi.org/10.1017/S0954102022000086>

636 Grabherr, M.G., Haas, B.J., Yassour, M., Levin, J.Z., Thompson, D.A., Amit, I., Adiconis, X., Fan,
637 L., Raychowdhury, R., Zeng, Q., Chen, Z., Mauceli, E., Hacohen, N., Gnirke, A., Rhind, N.,
638 Di Palma, F., Birren, B.W., Nusbaum, C., Lindblad-Toh, K., Friedman, N., Regev, A., 2011.
639 Full-length transcriptome assembly from RNA-Seq data without a reference genome. *Nature*
640 *Biotechnology* 29, 644–652. <https://doi.org/10.1038/nbt.1883>

641 Gu, B., Yang, T., Liu, X., Shen, H., 2019. Transcriptomic Analysis of the *Onchidium reevesii*
642 Central Nervous System in Response to Cadmium. *Frontiers in Marine Science* 6, 547.
643 <https://doi.org/10.3389/fmars.2019.00547>

644 Hao, T., Gao, Y., Li, Z.-C., Zhou, X.-X., Bing, Y., 2023. Size-Dependent Uptake and Depuration of
645 Nanoplastics in Tilapia (*Oreochromis niloticus*) and Distinct Intestinal Impacts. *Environmental*
646 *Science and Technology* 57, 2804–2812.
647 <https://doi.org/https://doi.org/10.1021/acs.est.2c08059>

648 Haynes, V.N., Ward, J.E., Russell, B.J., Agrios, A.G., 2017. Photocatalytic effects of titanium
649 dioxide nanoparticles on aquatic organisms Current knowledge and suggestions for future
650 research. *Aquatic Toxicology* 185, 138–148. <https://doi.org/10.1016/j.aquatox.2017.02.012>

651 Husmann, G., Abele, D., Rosenstiel, P., Clark, M.S., Kraemer, L., Philipp, E.E.R., 2014. Age-
652 dependent expression of stress and antimicrobial genes in the hemocytes and siphon tissue of
653 the Antarctic bivalve, *Laternula elliptica*, exposed to injury and starvation. *Cell Stress and*
654 *Chaperones* 19, 15–32. <https://doi.org/10.1007/s12192-013-0431-1>

- 655 Isobe, A., Uchiyama-Matsumoto, K., Uchida, K., Tokai, T., 2017. Microplastics in the Southern
656 Ocean. *Marine Pollution Bulletin* 114, 623–626.
657 <https://doi.org/10.1016/j.marpolbul.2016.09.037>
- 658 Jeong, C.B., Kang, H.M., Byeon, E., Kim, M.S., Ha, S.Y., Kim, M., Jung, J.H., Lee, J.S., 2021.
659 Phenotypic and transcriptomic responses of the rotifer *Brachionus koreanus* by single and
660 combined exposures to nano-sized microplastics and water-accommodated fractions of crude
661 oil. *Journal of Hazardous Materials* 416, 125703.
662 <https://doi.org/10.1016/j.jhazmat.2021.125703>
- 663 Jeyavani, J., Sibiya, A., Gopi, N., Mahboob, S., Riaz, M.N., Vaseeharan, B., 2022. Dietary
664 consumption of polypropylene microplastics alter the biochemical parameters and histological
665 response in freshwater benthic mollusc *Pomacea paludosa*. *Environmental Research* 212,
666 113370. <https://doi.org/10.1016/j.envres.2022.113370>
- 667 Jovanovic, B., Ji, T., Palic, D., 2011. Gene expression of zebrafish embryos exposed to titanium
668 dioxide nanoparticles and hydroxylated fullerenes. *Ecotoxicology and Environmental Safety*
669 74, 1518–1525. <https://doi.org/10.1016/j.ecoenv.2011.04.012>
- 670 Kallio, H., Hilvo, M., Rodriguez, A., Lappalainen, E., Lappalainen, A., Parkkila, S., 2010. Global
671 transcriptional response to carbonic anhydrase IX deficiency in the mouse stomach. *BMC*
672 *Genomics* 11, 397. <https://doi.org/http://www.biomedcentral.com/1471-2164/11/397>
- 673 Kelly, A., Lannuzel, D., Rodemann, T., Meiners, K.M., Auman, H.J., 2020. Microplastic
674 contamination in east Antarctic sea ice. *Marine Pollution Bulletin* 154, 111130.
675 <https://doi.org/10.1016/j.marpolbul.2020.111130>
- 676 Krasnobaev, A., Ten Dam, G., Boerrigter-Eenling, R., Peng, F., Van Leeuwen, S.P.J., Morley, S.A.,
677 Peck, L.S., Van Den Brink, N.W., 2020. Legacy and Emerging Persistent Organic Pollutants in
678 Antarctic Benthic Invertebrates near Rothera Point, Western Antarctic Peninsula.
679 *Environmental Science and Technology* 54, 2763–2771.
680 <https://doi.org/10.1021/acs.est.9b06622>
- 681 Kulasza, M., Skuza, L., 2021. Changes of Gene Expression Patterns from Aquatic Organisms
682 Exposed to Metal Nanoparticles. *International journal of environmental research and public*
683 *health* 18, 8361. <https://doi.org/https://doi.org/10.3390/ijerph18168361>
- 684 Labille, J., Slomberg, D., Catalano, R., Robert, S., Apers-Tremelo, M.L., Boudenne, J.L., Manasfi,
685 T., Radakovitch, O., 2020. Assessing UV filter inputs into beach waters during recreational
686 activity: A field study of three French Mediterranean beaches from consumer survey to water
687 analysis. *Science of the Total Environment* 706, 136010.
688 <https://doi.org/10.1016/j.scitotenv.2019.136010>
- 689 Lacerda, A., Rodrigues, L., van Sebille, E., Rodrigues, F., Ribeiro, L., Secchi, E., Kessler, F.,

690 Proietti, M., 2019. Plastics in sea surface waters around the Antarctic Peninsula. Scientific
691 Reports 9. <https://doi.org/10.1038/s41598-019-40311-4>

692 Lee, S., Kim, S.M., Lee, R.T., 2013. Thioredoxin and Thioredoxin Target Proteins : From
693 Molecular Mechanisms to Functional Significance. *Antioxidants & Redox Signaling* 18, 1165–
694 1207. <https://doi.org/10.1089/ars.2011.4322>

695 Leistenschneider, C., Burkhardt-Holm, P., Mani, T., Primpke, S., Taubner, H., Gerdts, G., 2021.
696 Microplastics in the Weddell Sea (Antarctica): A Forensic Approach for Discrimination
697 between Environmental and Vessel-Induced Microplastics. *Environmental Science and*
698 *Technology* 55, 15900–15911. <https://doi.org/10.1021/acs.est.1c05207>

699 Li, J., Lusher, A.L., Rotchell, J.M., Deudero, S., Turra, A., Bråte, I.L.N., Sun, C., Shahadat
700 Hossain, M., Li, Q., Kolandhasamy, P., Shi, H., 2019. Using mussel as a global bioindicator of
701 coastal microplastic pollution. *Environmental Pollution* 244, 522–533.
702 <https://doi.org/10.1016/j.envpol.2018.10.032>

703 Li, Z., Feng, C., Pang, W., Tian, C., Zhao, Y., 2021. Nanoplastic-Induced Genotoxicity and
704 Intestinal Damage in Freshwater Benthic Clams (*Corbicula fluminea*): Comparison with
705 Microplastics. *ACS Nano* 15, 9469–9481. <https://doi.org/10.1021/acsnano.1c02407>

706 Lister, K.N., Lamare, M.D., Burritt, D.J., 2015. Oxidative damage and antioxidant defence
707 parameters in the Antarctic bivalve *Laternula elliptica* as biomarkers for pollution impacts.
708 *Polar Biology* 38, 1741–1752. <https://doi.org/10.1007/s00300-015-1739-3>

709 Liu, Z., Li, Y., Edgar, P., Huang, Y., Yang, Y., Zhao, Y., 2021. Polystyrene nanoplastic induces
710 oxidative stress , immune defense , and glycometabolism change in *Daphnia pulex*:
711 Application of transcriptome profiling in risk assessment of nanoplastics. *Journal of Hazardous*
712 *Materials* 402, 123778. <https://doi.org/10.1016/j.jhazmat.2020.123778>

713 Livak, K.J., Schmittgen, T.D., 2001. Analysis of relative gene expression data using real-time
714 quantitative PCR and the 2- $\Delta\Delta$ CT method. *Methods* 25, 402–408.
715 <https://doi.org/10.1006/meth.2001.1262>

716 Love, M.I., Huber, W., Anders, S., 2014. Moderated estimation of fold change and dispersion for
717 RNA-seq data with DESeq2. *Genome Biology* 15, 550. <https://doi.org/10.1186/s13059-014-0550-8>

719 Madsen, J., Mollenhauer, J., Holmskov, U., 2010. Review: Gp-340/DMBT1 in mucosal innate
720 immunity. *Innate Immunity* 16, 160–167. <https://doi.org/10.1177/1753425910368447>

721 Mardian, E.B., Bradley, R.M., Duncan, R.E., 2015. The HRASLS (PLA / AT) subfamily of
722 enzymes. *Journal of Biomedical Science* 22, 99. <https://doi.org/10.1186/s12929-015-0210-7>

723 Marín, I., van Egmond, W.N., van Haastert, P.J.M., 2008. The Roco protein family: a functional
724 perspective. *The FASEB journal* 22, 3103–3110. <https://doi.org/10.1096/fj.08->

725 111310
726 Materić, D., Kjær, H.A., Vallelonga, P., Tison, J.L., Röckmann, T., Holzinger, R., 2022.
727 Nanoplastics measurements in Northern and Southern polar ice. *Environmental Research* 208,
728 112741. <https://doi.org/10.1016/j.envres.2022.112741>
729 Middelbeek, J., Clark, K., Leeuwen, F.N. Van, 2010. The alpha-kinase family: an exceptional
730 branch on the protein kinase tree. *Cellular and Molecular Life Science* 67, 875–890.
731 <https://doi.org/10.1007/s00018-009-0215-z>
732 Milan, M., Ferrareso, S., Ciofi, C., Chelazzi, G., Carrer, C., Ferrari, G., Pavan, L., Patarnello, T.,
733 Bargelloni, L., 2013. Exploring the effects of seasonality and chemical pollution on the
734 hepatopancreas transcriptome of the Manila clam. *Molecular Ecology* 22, 2157–2172.
735 <https://doi.org/10.1111/mec.12257>
736 Munari, C., Infantini, V., Scoponi, M., Rastelli, E., Corinaldesi, C., Mistri, M., 2017. Microplastics
737 in the sediments of Terra Nova Bay (Ross Sea, Antarctica). *Marine Pollution Bulletin* 122,
738 161–165. <https://doi.org/10.1016/j.marpolbul.2017.06.039>
739 Murano, C., Bergami, E., Liberatori, G., Palumbo, A., Corsi, I., 2021. Interplay Between
740 Nanoplastics and the Immune System of the Mediterranean Sea Urchin *Paracentrotus lividus*.
741 *Frontiers in Marine Science* 8, 647394.
742 <https://doi.org/https://doi.org/10.3389/fmars.2021.647394>
743 Nair, P.M.G., Park, S.Y., Lee, S., Choi, J., 2011. Differential expression of ribosomal protein gene,
744 gonadotrophin releasing hormone gene and Balbiani ring protein gene in silver nanoparticles
745 exposed *Chironomus riparius*. *Aquatic Toxicology* 101, 31–37.
746 <https://doi.org/10.1016/j.aquatox.2010.08.013>
747 Olalla, A., Moreno, L., Valcárcel, Y., 2020. Prioritisation of emerging contaminants in the northern
748 Antarctic Peninsula based on their environmental risk. *Science of the Total Environment* 742,
749 140417. <https://doi.org/10.1016/j.scitotenv.2020.140417>
750 Oomen, R.A., Hutchings, J.A., 2017. Transcriptomic responses to environmental change in fishes:
751 Insights from RNA sequencing. *Facets* 2, 610–641. <https://doi.org/10.1139/facets-2017-0015>
752 Patro, R., Duggal, G., Love, M.I., Irizarry, R.A., Kingsford, C., 2017. Salmon provides fast and
753 bias-aware quantification of transcript expression. *Nature Methods* 14, 417–419.
754 <https://doi.org/10.1038/nmeth.4197>
755 Paul-Pont, I., Lacroix, C., González Fernández, C., Hégaret, H., Lambert, C., Le Goïc, N., Frère, L.,
756 Cassone, A.L., Sussarellu, R., Fabioux, C., Guyomarch, J., Albentosa, M., Huvet, A., Soudant,
757 P., 2016. Exposure of marine mussels *Mytilus spp.* to polystyrene microplastics: Toxicity and
758 influence on fluoranthene bioaccumulation. *Environmental Pollution* 216, 724–737.
759 <https://doi.org/10.1016/j.envpol.2016.06.039>

- 760 Peck, L.S., 2018. Antarctic marine biodiversity: Adaptations, environments and responses to
761 change. *Oceanography and Marine Biology: An Annual Review* 56, 105–236.
762 <https://doi.org/10.1201/9780429454455-3>
- 763 Perfetti-Bolaño, A., Muñoz, K., Kolok, A.S., Araneda, A., Barra, R.O., 2022. Analysis of the
764 contribution of locally derived wastewater to the occurrence of Pharmaceuticals and Personal
765 Care Products in Antarctic coastal waters. *The Science of the total environment* 851, 158116.
766 <https://doi.org/https://doi.org/10.1016/j.scitotenv.2022.158116>
- 767 Reid, N.M., Whitehead, A., 2016. Functional genomics to assess biological responses to marine
768 pollution at physiological and evolutionary timescales: Toward a vision of predictive
769 ecotoxicology. *Briefings in Functional Genomics* 15, 358–364.
770 <https://doi.org/10.1093/bfpg/elv060>
- 771 Rota, E., Bergami, E., Corsi, I., Bargagli, R., 2022. Macro- and Microplastics in the Antarctic
772 Environment : Ongoing Assessment and Perspectives. *Environments* 9, 93.
773 <https://doi.org/https://doi.org/10.3390/environments9070093>
- 774 Sears, R.M., Roux, K.J., 2020. Diverse cellular functions of barrier-to-autointegration factor and its
775 roles in disease. *The Company of Biologists* 133, jcs246546.
776 <https://doi.org/10.1242/jcs.246546>
- 777 Sfriso, A.A., Tomio, Y., Rosso, B., Gambaro, A., Sfriso, A., Corami, F., Rastelli, E., Corinaldesi,
778 C., Mistri, M., Munari, C., 2020. Microplastic accumulation in benthic invertebrates in Terra
779 Nova Bay (Ross Sea, Antarctica). *Environment International* 137, 105587.
780 <https://doi.org/10.1016/j.envint.2020.105587>
- 781 Shao, Z., Guagliardo, P., Jiang, H., Wang, W., 2021. Intra- and Intercellular Silver Nanoparticle
782 Translocation and Transformation in Oyster Gill Filaments: Coupling Nanoscale Secondary
783 Ion Mass Spectrometry and Dual Stable Isotope Tracing Study. *Environmental Science and
784 Technology* 55, 433–446. <https://doi.org/10.1021/acs.est.0c04621>
- 785 Simão, F.A., Waterhouse, R.M., Ioannidis, P., Kriventseva, E. V., Zdobnov, E.M., 2015. BUSCO:
786 Assessing genome assembly and annotation completeness with single-copy orthologs.
787 *Bioinformatics* 31, 3210–3212. <https://doi.org/10.1093/bioinformatics/btv351>
- 788 Sleight, V.A., Thorne, M.A.S., Peck, L.S., Clark, M.S., 2015. Transcriptomic response to shell
789 damage in the Antarctic clam, *Laternula elliptica*: Time scales and spatial localisation. *Marine
790 Genomics* 20, 45–55. <https://doi.org/10.1016/j.margen.2015.01.009>
- 791 Suaria, G., Perold, V., Lee, J.R., Lebouard, F., Aliani, S., Ryan, P.G., 2020. Floating macro- and
792 microplastics around the Southern Ocean: Results from the Antarctic Circumnavigation
793 Expedition. *Environment International* 136, 105494.
794 <https://doi.org/10.1016/j.envint.2020.105494>

- 795 Sun, T.Y., Bornhöft, N.A., Hungerbühler, K., Nowack, B., 2016. Dynamic Probabilistic Modeling
796 of Environmental Emissions of Engineered Nanomaterials. *Environmental Science and*
797 *Technology* 50, 4701–4711. <https://doi.org/10.1021/acs.est.5b05828>
- 798 Szopińska, M., Potapowicz, J., Jankowska, K., Luczkiewicz, A., Svahn, O., Björklund, E., Nannou,
799 C., Lambropoulou, D., Polkowska, Ż., 2022. Pharmaceuticals and other contaminants of
800 emerging concern in Admiralty Bay as a result of untreated wastewater discharge : Status and
801 possible environmental consequences. *Science of the Total Environment* 835, 155400.
802 <https://doi.org/10.1016/j.scitotenv.2022.155400>
- 803 Teles, M., Reyes-lópez, F.E., Balasch, J.C., Tvarijonaviciute, A., Guimarães, L., Oliveira, M., Tort,
804 L., James, R.A., 2019. Toxicogenomics of Gold Nanoparticles in a Marine Fish : Linkage to
805 Classical Biomarkers. *Frontiers in Marine Science* 6, 147.
806 <https://doi.org/10.3389/fmars.2019.00147>
- 807 Teng, J., Zhao, J., Zhu, X., Shan, E., Zhang, C., Zhang, W., Wang, Q., 2021. Toxic effects of
808 exposure to microplastics with environmentally relevant shapes and concentrations:
809 Accumulation, energy metabolism and tissue damage in oyster *Crassostrea gigas*.
810 *Environmental Pollution* 269, 116169. <https://doi.org/10.1016/j.envpol.2020.116169>
- 811 Trevisan, R., Ranasinghe, P., Jayasundra, N., Di Giulio, R., 2022. Nanoplastics in Aquatic
812 Environments: Impacts on Aquatic Species and Interactions with Environmental Factors and
813 Pollutants. *Toxics* 10, 326. <https://doi.org/https://doi.org/10.3390/toxics10060326>
- 814 Truebano, M., Burns, G., Thorne, M.A.S., Hillyard, G., Peck, L.S., Skibinski, D.O.F., Clark, M.S.,
815 2010. Transcriptional response to heat stress in the Antarctic bivalve *Laternula elliptica*.
816 *Journal of Experimental Marine Biology and Ecology* 391, 65–72.
817 <https://doi.org/10.1016/j.jembe.2010.06.011>
- 818 Van Aerle, R., Lange, A., Moorhouse, A., Paszkiewicz, K., Ball, K., Johnston, B.D., Booth, T.,
819 Tyler, C.R., Santos, E.M., 2013. Molecular Mechanisms of Toxicity of Silver Nanoparticles in
820 Zebra fish Embryos. *Environmental Science and Technology* 47, 8005–8014.
821 <https://doi.org/dx.doi.org/10.1021/es401758d>
- 822 Waller, C.L., Griffiths, H.J., Waluda, C.M., Thorpe, S.E., Loaliza, I., Moreno, B., Pacherres, C.O.,
823 Hughes, K.A., 2017. Microplastics in the Antarctic marine system: An emerging area of
824 research. *Science of the Total Environment* 598, 220–227.
825 <https://doi.org/10.1016/j.scitotenv.2017.03.283>
- 826 Yeo, M.-K., Park, H.-G., 2012. Gene expression in zebrafish embryos following exposure to Cu-
827 doped TiO₂ and pure TiO₂ nanometer-sized photocatalysts. *Molecular & Cellular Toxicology*
828 8, 127–137. <https://doi.org/https://doi.org/10.1007/s13273-012-0016-6>
- 829 Zhang, X., Wen, H., Wang, H., Ren, Y., Zhao, J., Li, Y., 2017. RNA-Seq analysis of salinity stress

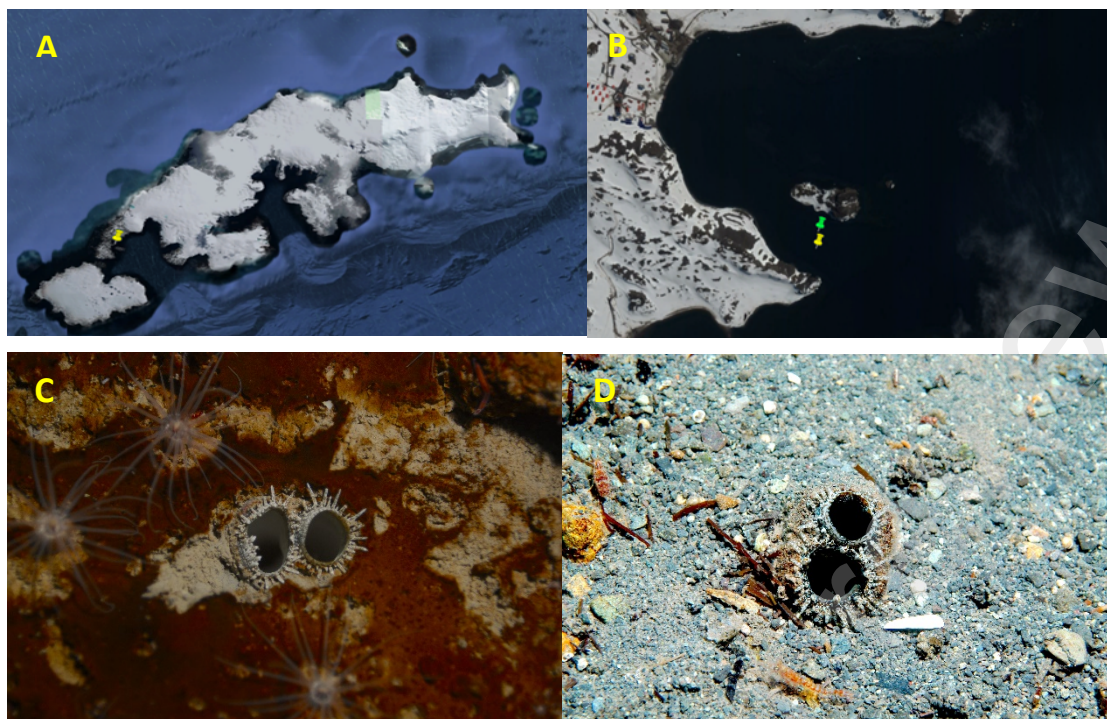
830 – responsive transcriptome in the liver of spotted sea bass (*Lateolabrax maculatus*). PLoS
831 ONE 12, e0173238. <https://doi.org/10.1371/journal.pone.0173238>

832 Zhao, C.-M., Wang, W.-X., 2012. Size-Dependent Uptake of Silver Nanoparticles in *Daphnia*
833 *magna*. Environmental Science and Technology 46, 11345–11351.
834 <https://doi.org/10.1021/es3014375>

835 Zheng, M., Lu, J., Zhao, D., 2018. Science of the Total Environment Effects of starch-coating of
836 magnetite nanoparticles on cellular uptake , toxicity and gene expression profiles in adult
837 zebra fish. Science of the Total Environment 622–623, 930–941.
838 <https://doi.org/10.1016/j.scitotenv.2017.12.018>

839 Zhou, Y., Li, Y., Lan, W., Jiang, H., Pan, K., 2022. Short-Term Exposure to MPs and DEHP
840 Disrupted Gill Functions in Marine Bivalves. Nanomaterials 12, 4077.
841 <https://doi.org/10.3390/nano12224077>

842



845

846

847 **Figure 1.** Sampling points where *Laternula elliptica* clams were collected on King George Island (A)
848 at Fildes Bay (B). The points correspond to geo-referential coordinates 62° 12' 17.32" S, 58° 56'
849 56.48" W and 62° 12' 19.34" S, 58° 56' 57.0052" W (C-D) Pictures of *L. elliptica* individuals in their
850 natural environment (photos from Dr. Ignacio Garrido).

851 **Table 1.** Sequencing, filters, alignments and assembly statistics of the present study using 32 paired-
852 ends samples.

Reads

Raw Reads	975 727 394
Filtered Reads	975 727 394
Total Aligned and counted reads	892 620 127
Aligned and counted reads (%)	91.48

Assembly

Total trinity transcripts	603954
Total trinity genes	279798
GC (%)	38.93
Total trinity transcripts After CD-Hit	251294
Total trinity genes After CD-Hit	222734
GC (%) After CD-Hit	38.26

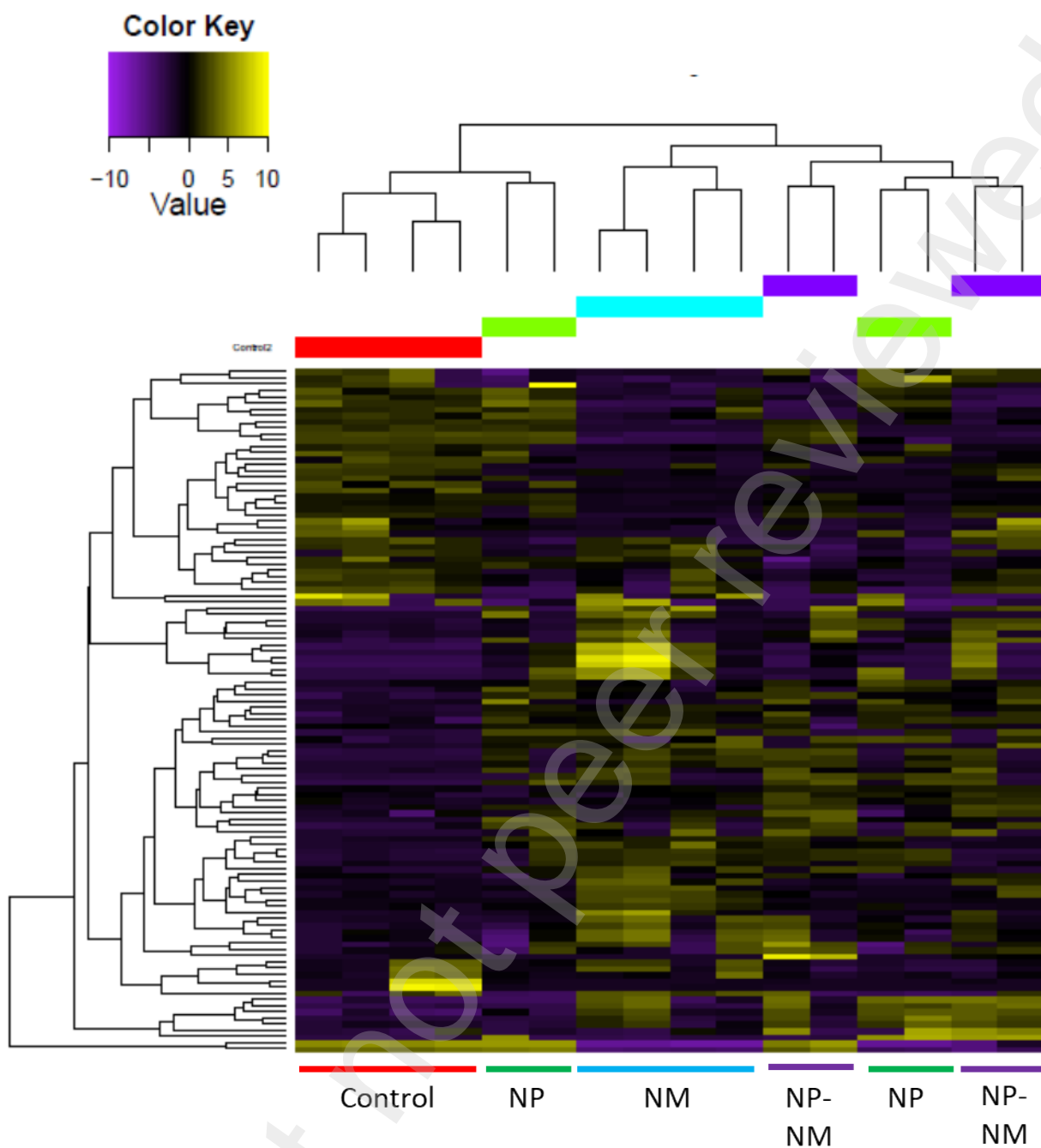
Assembly statistics After CD-Hit

N50	955
Median length (bp)	382
Average length (bp)	675.17

BUSCO statistics After CD-Hit

Total completeness (%)	99.4
Complete and single-copy (%)	92.4
Complete and duplicated (%)	7.0
Fragmented (%)	0.6
Missing (%)	0.0

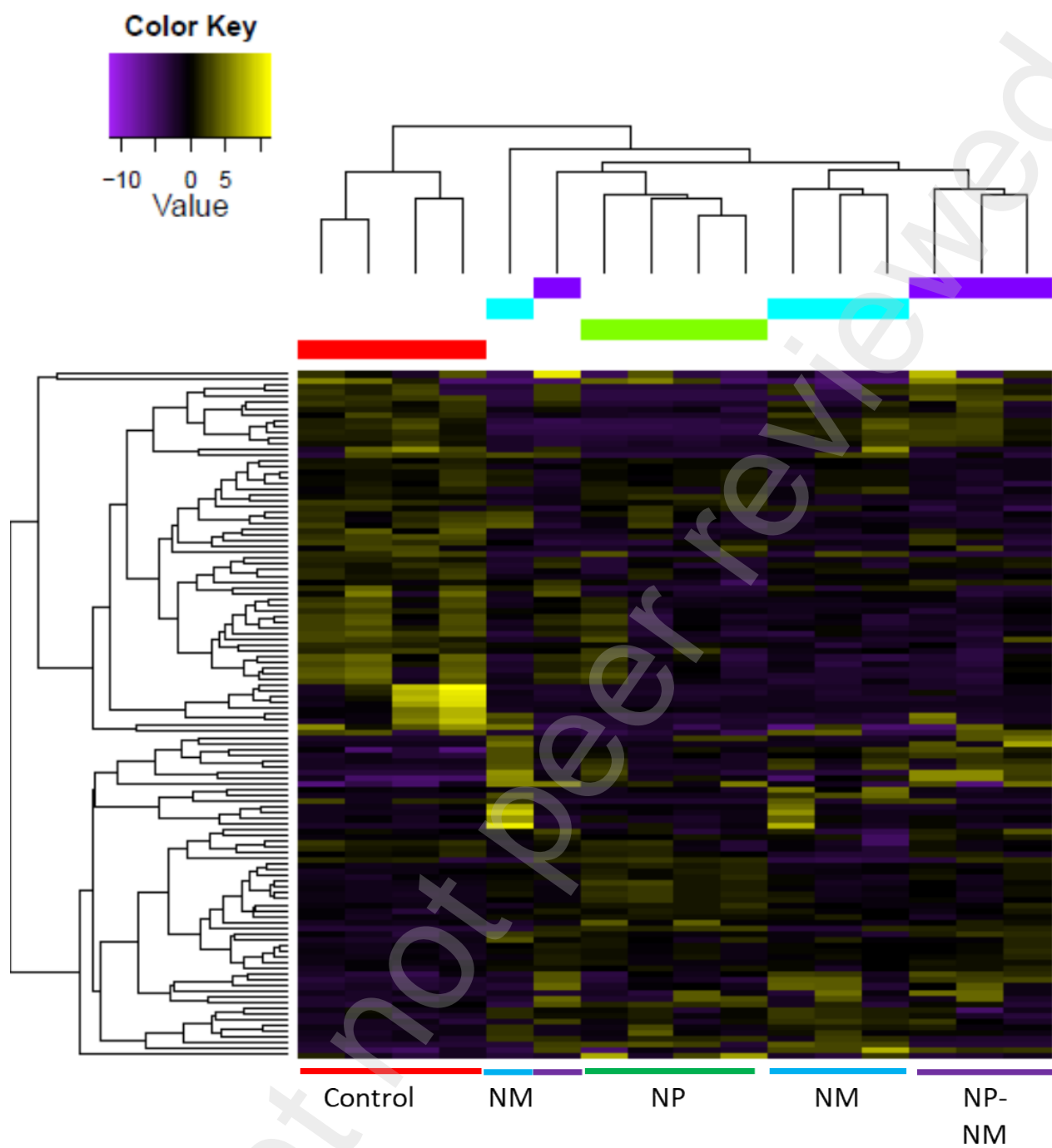
853



854

855 **Figure 2.** Heatmap of Differentially Expressed Genes revealing the clustering of the control group
 856 (Control, in red), and treatments exposed to 5 $\mu\text{g/ml}$ nanoparticles: PS-COOH NP (NP, in green), n-
 857 TiO_2 (NM, in blue) and combined exposure (NP-NM, in violet).

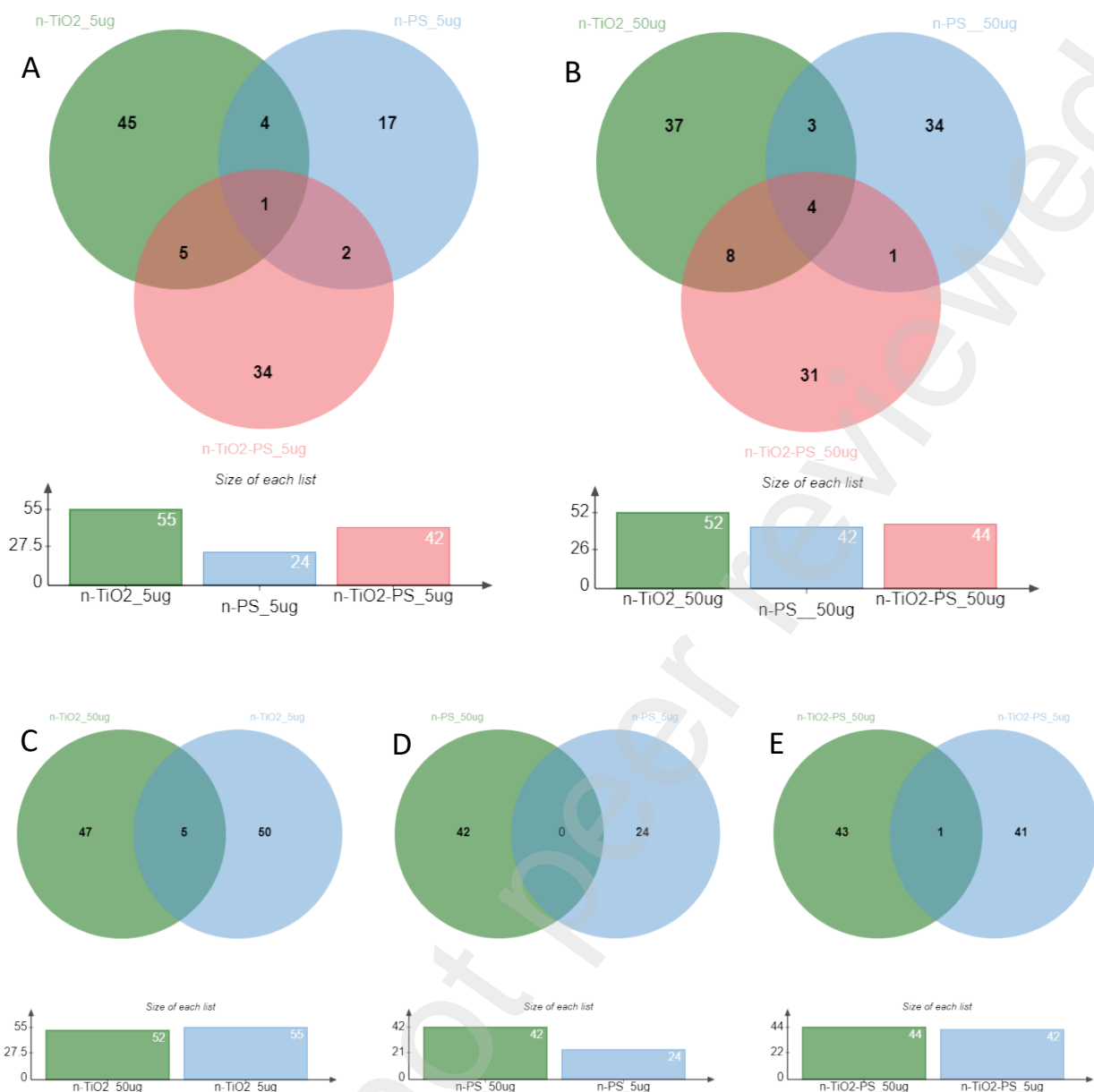
858



859

860 **Figure 3.** Heatmap of Differentially Expressed Genes revealing the clustering of control group
 861 (Control, in red), and treatments exposed to 50 $\mu\text{g/ml}$ nanoparticles: PS-COOH NP (NP, in green),
 862 n-TiO₂ (NM, in blue) and combined exposure (NP-NM, in violet).

863



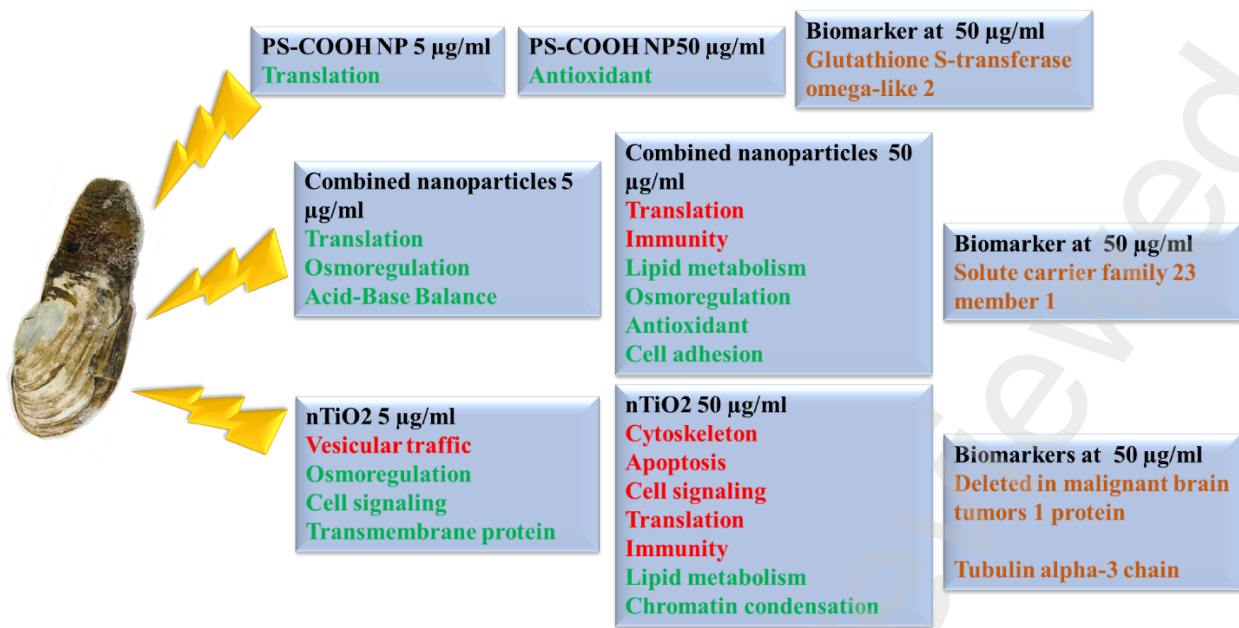
864
865

866

867 **Figure 4.** Venn diagrams showing shared Differentially Expressed Genes (DEG) when comparing
 868 individuals exposed to control end experimental conditions at 5 µg/ml (A) and 50 µg/ml (B). The
 869 green circles represent the n-TiO₂ conditions, the blue ones the PS-COOH NP conditions and the pink
 870 ones the co-exposure to both nanoparticles. The overlaps of circles represent the shared DEG.
 871 Barplots show DEG numbers by conditions with the same colors of circles. Venn diagrams showing
 872 shared transcripts between pair of conditions for n-TiO₂ (A), PS-COOH NP (B) and combined
 873 exposure (C). Green circles represent the 50 µg/ml treatments for each pollutant and the blue ones
 874 represent the 5 µg/ml treatments. The overlaps of the circles represent the shared transcripts. Barplots
 875 show transcript numbers by conditions.

876

877



878

879 **Figure 5.** Molecular effects of the exposure to PS-COOH NP and/or n-TiO₂ in the Antarctic soft clam
 880 *L. elliptica* at 5 and 50 µg/ml. Molecular functions with up-regulated transcripts are shown in green
 881 and down-regulated ones in green. The molecular biomarkers validated with eight clams are marked
 882 in brown.

883

884